CONF-790901--4

LA-UR-79-662

TITLE: THE DESIGN AND PERFORMANCE OF A MAGNETIC REFRIGERATOR AND HEAT ENGINE

MASTER

AUTHOR(S): J. A. Barclay, W.A. Steyert, and D. R. Zrudsky

SUBMITTED TO: XVth International Congress of Refrigeration

THE DESIGN AND PERFORMANCE OF A MAGNETIC REFRIGERATOR AND HEAT ENGINE*

J. A. Barclay, W. A. Steyert, and D. R. Zrudsky**
Los Alamos Scientific Laboratory, Los Alamos, NM 87545

1. INTRODUCTION

In 1918 Weiss and Piccard /1/ reported on "a new magnetocaloric phenomenon" in which they described the increase in temperature of nickel caused by a magnetic field. A full investigation of the magnetocaloric effect of nickel was published in 1926 /2/ followed by a similar study for iron in 1934. /3/ However, the discovery of the magnetocaloric effect was preceded by an interest in practical refrigerators and engines based on the ferromagnetic-paramagnetic transition as illustrated by patents from Edison /4/ and Tesla. /5/ Actual devices didn't appear until recently when high field magnets and pure rare earth elements such as gadolinium became available. /6-10/ In this paper we report on a magnetic refrigerator/heat engine which we have designed and built.

2. PRINCIPLES OF MAGNETIC REFRIGERATORS/HEAT ENGINES

Thermomagnetic refrigerators or heat engines utilize the temperature and field dependence of the magnetic entropy either to extract heat from a sink or to convert heat from a source into mechanical energy. The cycle(s) can be easily shown on an entropy-temperature diagram such as Fig. 1. A magnetic Brayton refrigeration cycle is shown by the path of the solid arrows. Starting at temperature T_C and zero magnetic field, the magnetic working material is heated by heat exchange with a counterflowing fluid up to T_H. At this point it enters the magnetic field and is heated by the magnetocaloric effect to $T_H + \Delta_H$. The return heat exchange (regeneration) path is executed in the magnetic field until the working material is cooled to $T_C + \Delta_C$ at which point it is removed from the field. The magnetic

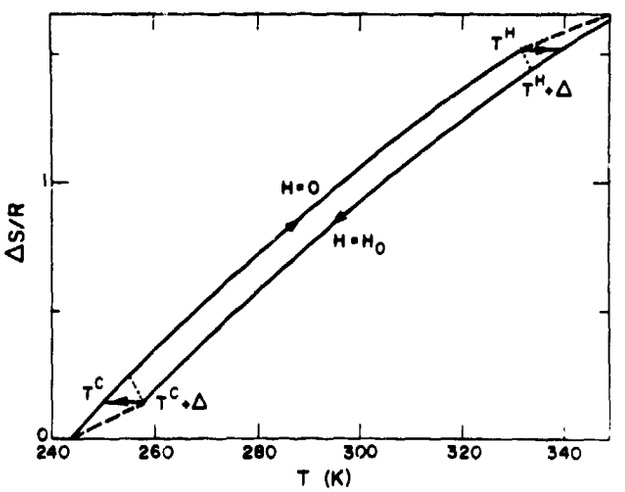

Fig. 1. The entropy-temperature diagram (R is the gas constant) showing the thermodynamic cycle executed by the magnetic material.

*Work performed under the auspices of the U.S. Department of Energy for the Electric Power Research Institute.
**Professor D. R. Zrudsky is on sabbatical leave from the University of Toledo, Toledo, Ohio 43606.

material cools to T_C by the magnetocaloric effect and the cycle is complete. The heat exchange fluid enters the external cold heat exchanger at T_C and leaves at $T_C + \Delta_C$ thus extracting heat from the refrigeration load. The fluid also enters the hot heat exchanger at $T_H + \Delta_H$ and leaves at T_H thus dumping heat into the hot reservoir. At least two different designs which execute this cycle have been reported. /7 9/ The first of these is a reciprocating device which uses gadolinium metal as the working material and alcohol or water as the regenerator fluid. A schematic diagram of this device is shown in Fig. 2. The operation is similar to that described in Fig. 1 with heat being transferred to the hot sink as the field is applied, followed by regeneration in the field, then, heat being removed from the cold source as the field is removed, followed by regeneration in zero field. Up to an 80°C temperature gradient in the regenerator has been achieved using a 7 Tesla field. /8/

The second design is a rotating wheel device which also uses gadolinium metal as the working material. A schematic of this device is shown in Fig. 3. The refrigeration cycle is exactly like that described in Fig. 1. The gadolinium metal is porous so that the regenerator fluid (water or alcohol) can be circulated in the opposite direction to the motion of the wheel. The top one-third and bottom one-third of the wheel form counterflow heat exchangers. The fluid flows through the

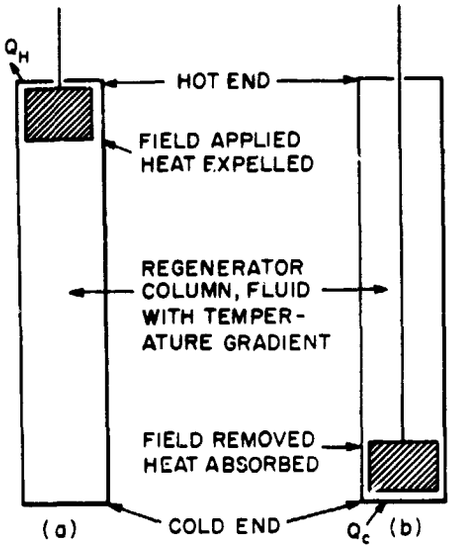

Fig. 2. A schematic of a reciprocating magnetic refrigerator.

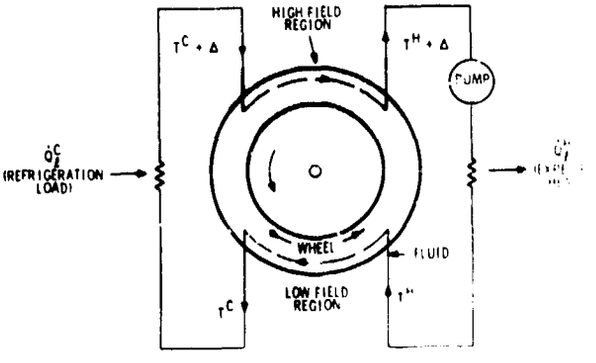

Fig. 3. A schematic of a wheel-shaped magnetic refrigerator in the refrigerator mode.

cold and hot external heat exchangers picking up and expelling the corresponding amounts of heat. Since the fluid and the working material are always very close to the same temperature, very little entropy is created and the design should be extremely efficient. The device we are about to describe in more detail is based on this second design.

3. MAGNETIC WHEEL REFRIGERATOR/HEAT ENGINE DESIGN

The overall schematic of the magnetic wheel is shown in Fig. 4. The helium Dewar holds a NbTi superconducting racetrack-shaped magnet designed for 6 Tesla. The bottom of the Dewar has a recess which allows the top one-third of the gadolinium wheel to be in the high magnetic field. The bottom one-third of the wheel is in a much lower magnetic field (0.1-1 Tesla). The external heat exchangers and fluid pump are also shown in Fig. 4.

Some special design problems are encountered in forcing the fluid (water in our system) to flow (referring to Fig. 3) from upper left to upper right, clockwise against the counterclockwise wheel rotation. The design has to prevent fluid flow in the counterclockwise direction of wheel rotation, for instance in the "adiabatic section" from upper left to lower left.

Figures 5-6 show the details of the wheel design. The rotating wheel (Fig. 5) has 18 fluid-tight compartments, each containing a porous gadolinium pressing. The wheel is surrounded by a housing containing many small, annular fluid chambers. The fluid enters a compartment in the wheel from a chamber in the housing through a wheel entrance slot. In each compartment, the fluid flows clockwise, through the porous gadolinium, exiting the compartment and entering the next clockwise compartment. The neoprene lip seals prevent the flow of fluid back to the adjacent counterclockwise compartment. Thus, if the velocity of fluid flow through each compartment is sufficiently rapid, the net fluid flow is clockwise as shown in the upper and lower thirds of the schematic wheel of Fig. 3.

Although the compartmented wheel design provides flow in the clockwise direction, it does not, at first glance, entirely prevent flow in the counterclockwise direction. Some of the fluid introduced at the housing entrance ports (upper left and lower right in Fig. 5) is entrained in the wheel and moves counterclockwise with it, through the adiabatic sections on the left and right of the wheel. The gadolinium in the wheel has about 40% void fraction and can entrain this amount of water. This thermal load on the magnetocaloric effect in the gadolinium reduces Δ, the temperature change in the adiabatic sections (the water specific heat equals the gadolinium specific heat at a 32/68 water/gadolinium volume ratio). The entrained fluid problem is solved by allowing a controlled volume of fluid to flow

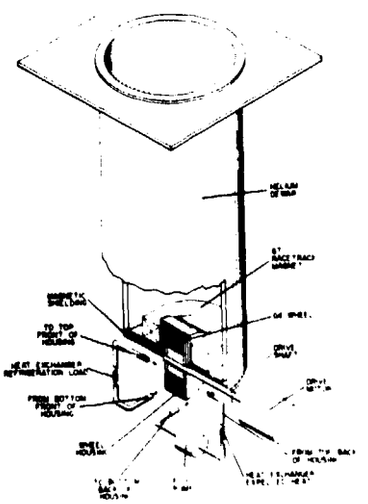

Fig. 4. Overall view of the magnetic refrigerator.

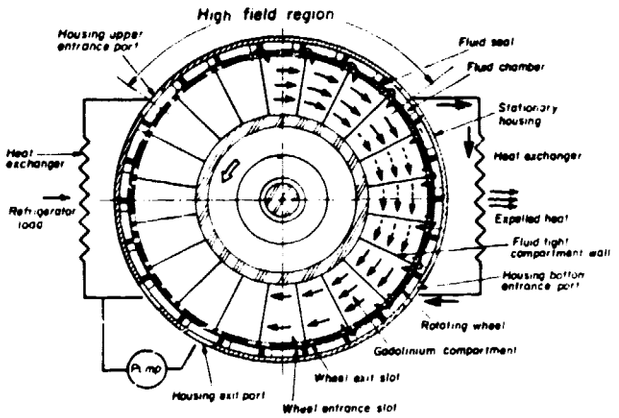

Fig. 5. A view showing flow details in the housing and wheel.

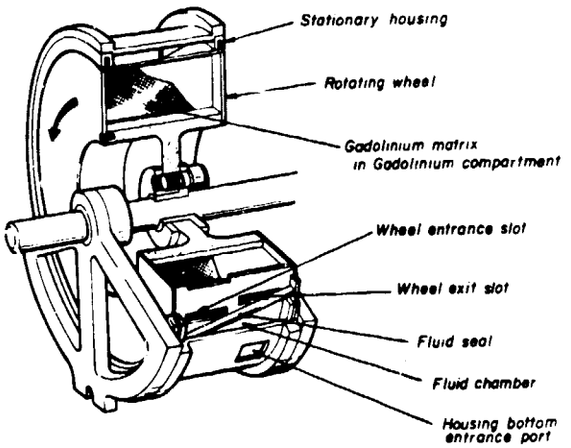

Fig. 6. Cutaway of wheel and housing showing orifices in compartments, seals, and mounting.

clockwise through the adiabatic sections of the wheel (where no flow is shown in Fig. 3). This small flow equals the entrained fluid flow, so that there is no net flow (the water molecules in the left and right sections are not moving in the laboratory frame of reference, even though they are entrained in the porous gadolinium).

4. RESULTS AND DISCUSSION

Flow measurements with no magnetic field

The pressure drops in the wheel which was rotating at 0.1 Hz were measured as a function of water flow rate. Both of the external heat exchangers were closed off so the total flow was around the entire wheel. Both electronic and Bourdon type transducers were used for the pressure and orifice flow meters. The results of these measurements are close to the predicted pressure drop, ΔP, which is dominated by the gadolinium and orifice pressure drops. /11/ The predicted pressure drop is given by

$$\Delta P(kPa) = 130\ \dot{V} + 69\ \dot{V}^2 \quad ,$$

where $\dot{V}$ is the volume flow rate in deciliters/s. The linear term comes from the gadolinium and the quadratic term from the orifices.

Refrigeration runs with a 3 tesla magnetic field

The magnet was charged to 80 A (3.0 Tesla) and the wheel was rotated at 0.1 Hz while the temperature was monitored using thermocouples. The flow rate was varied until the maximum temperature difference between the hot and cold side of the wheel was achieved. The maximum ΔT measured was 9°C. The wheel rotation rate was increased to 0.2 Hz while the water flow was varied in many ways, but ΔT did not increase above 9°C. The most important results of this initial experiment are that with the hot and cold heat exchangers operating, we were able to pump 500 W across a 7°C temperature span at 0.1 Hz. We also were able to run the wheel as a heat engine by running cold water through the hot side heat exchanger while heating the cold side exchanger. The torque produced was at least 5.6 Nm (50 in.-lbs) at 0.1 Hz for a power of 4 W. Although this is not a large net power output, the small temperature difference between the hot and cold baths make the ideal Carnot efficiency extremely low so the fact that it operated as a heat engine is significant.

Analysis of results

We have reanalyzed many of our design calculations in an attempt to explain these initial results. A summary of these calculations is shown below.

1. Internal temperature oscillations

The temperature oscillations in the water measured at the top and bottom of the wheel had two frequencies, one of magnitude 1°C peak to peak with a 1 cycle period; and one of 0.5°C magnitude peak to peak with a 1/18 cycle period. The cause of these temperature oscillations is a water flow variation through the gadolinium (which is rotating at constant speed). The oscillation of 1 cycle period is probably associated with the flow impedance variation in the gadolinium segments around the wheel. This impedance variation was made as small as possible by selecting individual segments according to the ratio of pressure drop to density. The smaller, more rapid oscillations are associated with the orifices of each compartment since there are 18 compartments.

These temperature oscillations will cause entropy creation since the gadolinium is always at a slightly different temperature and the water is mixed in every housing chamber. The entropy created can be estimated by using

$$\Delta S = dQ\ \Delta T/2T^2 \quad ,$$

where ΔS is the irreversible entropy produced, dQ is the heat flow between the two bodies initially ΔT apart in temperature with a mean temperature T. This formula is an excellent approximation for $\Delta T/T << 1$ and equal thermal masses which are the conditions that we have. Using the numbers for the wheel, the Gd-water mixing for 2/3 of the wheel gives $\dot{\Delta S}_{irr} = 0.005$ W/K. The water-water mixing gives $\dot{\Delta S}_{irr} = 0.028$ W/K for 12 compartments. Neither of these mechanisms gives very much irreversible entropy production because ΔT is so small.

2. Frictional losses

The frictional torque was measured for the wheel. An average result was 1.7 Nm (150 in.-lbs) at 0.2 Hz. The entropy production rate associated with this torque is $\dot{\Delta S} = 0.071$ W/K.

3. Parasitic heat leaks from ambient air

The pipes and hoses of the pumping system are exposed to air at ambient temperature. The heat leak associated with this system can be calculated by using the Dittus-Boelter equation to calculate the conductance, h, of the water in the pipes and hoses and a similar correlation for the conductance of the air to pipe or hose. The air to pipe impedance dominates completely and the entropy production rate for this heat leak into a ten-foot-long, 1/2-in.-diam pipe (hose) is $\dot{\Delta S} = 0.0004$ W/K.

4. Water flow fluctuations

The flow measurements obtained from the electronic transducers indicate a complex flow pattern with fluctuations of approximately 10%. We are presently

deciphering the flow pattern. However, all of our calculations indicate that the heat transfer unit, N_{tu}, of the counterflow heat exchange parts of the wheel should not be appreciably affected if the N_{tu} was large ($>>1$) initially. Since we designed for an N_{tu} of 180, the effect of flow fluctuations, leakage under the seals, and small flow inhomogeneity in the gadolinium should be negligible.

5. Pump losses and pressure drop through wheel

The water pump motor is rated at 250 W (1/3 of a horsepower) so the maximum loss from the pump and pressure drops around the wheel is 250 W. The maximum pressure drop loss around the wheel, $\dot{V}dP$, is 4.1×10^5 Pa (60 psi) (120 cm^3/s) (10^{-6}) = 50 W. The discrepancy between 50 W and 250 W suggests that the pump is extremely inefficient. We will take careful temperature measurements of the water before and after the pump to determine the exact loss. If the full 250 W is loss, then the entropy production rate is $\Delta\dot{S}$ = 0.83 W/K which is substantial.

6. Ideal refrigeration

From the entropy-temperature curves for gadolinium near room temperature the entropy change for a 3 Tesla to 0.5 Tesla magnetization or demagnetization is approximately 0.62 J/mole K. However, a careful check on the field profile indicates that ΔS should be reduced to 0.35 J/mole K for the adiabatic sections of the wheel. Therefore, the entropy change rate for refrigeration at 294 K and 0.2 Hz is

$$\Delta\dot{S} = \left(0.35 \frac{J}{\text{mole K}}\right)(14.6 \text{ moles})(0.2 \text{ Hz}) = 1.01 \text{ W/K}.$$

7. Summary of analysis

The ideal refrigeration entropy change rate is 1.01 W/K. The losses are listed below in order of magnitude:

(1)	Pump and pressure drop	0.83 W/K
(2)	Friction	0.07
(3)	Water-water mixing	0.03
(4)	Gd-water mixing	0.005
(5)	Parasitic heat leaks	0.0004
(6)	N_{tu} degradation	---

These losses give a total irreversible entropy production rate of 0.93 W/K which is close to the ideal entropy change rate.

5. CONCLUSIONS

The initial operation of the refrigerator/heat engine is very encouraging. Our analysis indicates that the magnetic field profile and inefficient water pump are the main reasons for the limited ΔT. Our next experiments will be performed with soft iron shielding to increase ΔH and also with a more efficient pump to reduce the heat load. The prognosis is very good.

The basic advantages of magnetic refrigerators/heat engines are that the energy density in the working material is very high, 25 kJ/ℓ of Gd at 300 K; the heat exchange is between a solid and a liquid which makes the regenerative stages of the cycle more efficient; and in some cases the expensive external heat exchangers could be eliminated. The disadvantage of magnetic refrigeration is that a superconducting magnet is required.

An example of an application at room temperature is a magnetic heat pump for utilization of low-grade waste heat such as in nuclear power plants. For applications such as this, where external heat exchangers may be eliminated, the economics look attractive. The prospects for magnetic refrigeration at low temperatures ($<$ 77K) look much better than at room temperature because the ratio of magnetic entropy to lattice entropy increases rapidly as the temperature decreases.

NOMENCLATURE

T	temperature, K
S	entropy, J/mole K
R	gas constant, 8.37 J/mole K
H	magnetic field intensity, A/m
Δ	temperature change under adiabatic magnetization or demagnetization
P	pressure, kPa
$\dot{V}$	volume flow rate, deciliters/s
dQ	heat, J
N_{tu}	heat transfer units, dimensionless.

REFERENCES

1. P. Weiss and Al. Piccard, Compt. rend. 166, 352 (1918).
2. P. Weiss and R. Forrer, Ann. Physique (10) 5, 153 (1926).
3. H. H. Potter, Proc. Roy. Soc. 146, 362 (1934).
4. T. Edison, British Patent 16,709 (1887).
5. N. Tesla, U.S. Patent 428,057 (1890).
6. R. E. Rosensweig, J. W. Nestor, and R. S. Timmins, A. I. Ch. E. - I. Chem. E., Symp. Series 5, 104 (1965).
7. G. V. Brown, J. Appl. Phys. 47, 3673 (1976).
8. G. V. Brown; preprint submitted to J. Appl. Phys. (1978).
9. W. A. Steyert, J. Appl. Phys. 49, 1216 (1978).
10. S. S. Rosenblum, W. P. Pratt, Jr., and W. A. Steyert, Los Alamos Scientific Laboratory report LA-6581 (1977).
11. J. A. Barclay, W. A. Steyert, and D. R. Zrudsky, Los Alamos Scientific Laboratory report LA-7654-PR (Nov. 1978).